Article

Discovery Medicine 2026; 38(210): 2178–2189
https://doi.org/10.24976/Discov.Med.202638210.170

RFC5 Targets CDK1 to Trigger Mitochondrial Fission and Facilitate Non-Small Cell Lung Cancer Progression

Yihui Huang[1], Yifan Dai[2,*], Zhaoyang Ruan[1], Zehai Xia[2], Quan Wang[3]

[1]Department of Tuberculosis, The Affiliated Hospital of Hangzhou Normal University, 310015 Hangzhou, Zhejiang, China
[2]Department of Respiratory and Critical Care Medicine, The Affiliated Hospital of Hangzhou Normal University, 310015 Hangzhou, Zhejiang, China
[3]Clinical Medical College, Hangzhou Normal University, 311121 Hangzhou, Zhejiang, China
*Correspondence: daiyifan6666@163.com (Yifan Dai)
Submitted: 20 May 2026 Revised: 10 June 2026 Accepted: 22 June 2026 Published: 23 July 2026

Background: The worldwide mortality from non-small cell lung cancer (NSCLC) is high, with a scarcity of effective therapies for advanced cases. Mitochondrial dynamics, particularly fission, is vital in cancer cell survival and progression. Herein, we examined how replication factor C 5 (RFC5), a DNA replication factor, influences mitochondrial fission and apoptosis in NSCLC.
Methods: Integrated bioinformatic analysis of the NSCLC-related dataset GSE19188 and apoptosis- and mitochondrial dynamics-related genes from GeneCards was performed to screen and identify RFC5 as a key candidate gene closely associated with NSCLC progression. We conducted *in vitro* functional validation and mechanistic dissection in A549 cells, including gain/loss-of-function experiments, cell proliferation, migration and invasion assays, flow cytometry, and co-immunoprecipitation to validate its oncogenic function and elucidate the underlying mechanism. Molecular docking between RFC5 and cyclin-dependent kinase 1 (CDK1), as well as rescue experiments with a dynamin-related protein 1 (DRP1) inhibitor (Mdivi-1), further delineated the signaling axis.
Results: RFC5 was identified as upregulated in NSCLC samples in GSE19188 ($p < 0.05$) and functional studies were conducted in A549 cells, and elevated RFC5 significantly promoted cell proliferation, migration, and invasion, while markedly blocking apoptosis ($p < 0.05$). Mechanistically, RFC5 physically interacted with CDK1, enhancing its expression. This RFC5-CDK1 axis facilitated DRP1-mediated mitochondrial fission, as evidenced by decreased mitochondrial membrane potential and altered expression of fission/fusion genes ($p < 0.05$). Importantly, the inhibitory effects of RFC5 silencing were reversed by CDK1 overexpression, whereas DRP1 inhibitor Mdivi-1 abolished the effects of CDK1 overexpression ($p < 0.05$).
Conclusion: Our findings unveil a potential RFC5-CDK1 signaling axis that may promote NSCLC cell progression *in vitro* by modulating mitochondrial fission and inhibiting apoptosis, highlighting a novel avenue for NSCLC intervention.

Keywords: non-small cell lung cancer; replication factor C 5; cyclin-dependent kinase 1; dynamin-related protein 1; mitochondrial fission

Introduction

Non-small cell lung cancer (NSCLC), accounting for nearly 85% of lung carcinomas, remains the leading cause of cancer-related mortality globally, highlighting the urgent need for more effective treatments [1]. A hallmark of malignant progression in NSCLC is evasion of apoptosis, which facilitates uncontrolled proliferation and poor prognosis [2,3]. Mitochondria, key regulators of cellular energy metabolism and survival, play a pivotal role in tumor development [4]. Emerging evidence suggests that mitochondrial metabolic function is critically involved in regulating tumor cell apoptosis, positioning mitochondrial targeting as a promising therapeutic approach [5].

Mitochondrial dynamics, governed by fission and fusion processes, maintain mitochondrial homeostasis and function [6]. Specifically, key GTPases (dynamin-related protein 1 (DRP1), Mitofusin 1/2 (MFN1/2), and optic atrophy protein 1 (OPA1)) regulate these processes [7,8,9]. The translocation of DRP1 to mitochondrial surfaces constitutes a pivotal prerequisite for mitochondrial fission, a process that is directly orchestrated by reversible phosphorylation events on DRP1 [10]. Notably, elevated DRP1 activity has been observed in multiple cancers, including NSCLC, where it facilitates mitochondrial division during mitosis and enhances tumor cell migration [11,12,13].

Through analysis of the NSCLC dataset GSE19188 (https://www.ncbi.nlm.nih.gov/gds/?term=GSE19188) and GeneCards (https://www.genecards.org/), we identified replication factor C 5 (RFC5), a gene associated with apoptosis and mitochondrial dynamics in NSCLC. As a primer recognition factor for DNA polymerase, RFC5 potentially orchestrates multiple facets of malignant progression, including cancer cell proliferation, invasion, and metastasis [14]. RFC5 is significantly upregulated in tumor tissues and correlates with aggressive clinicopathological features

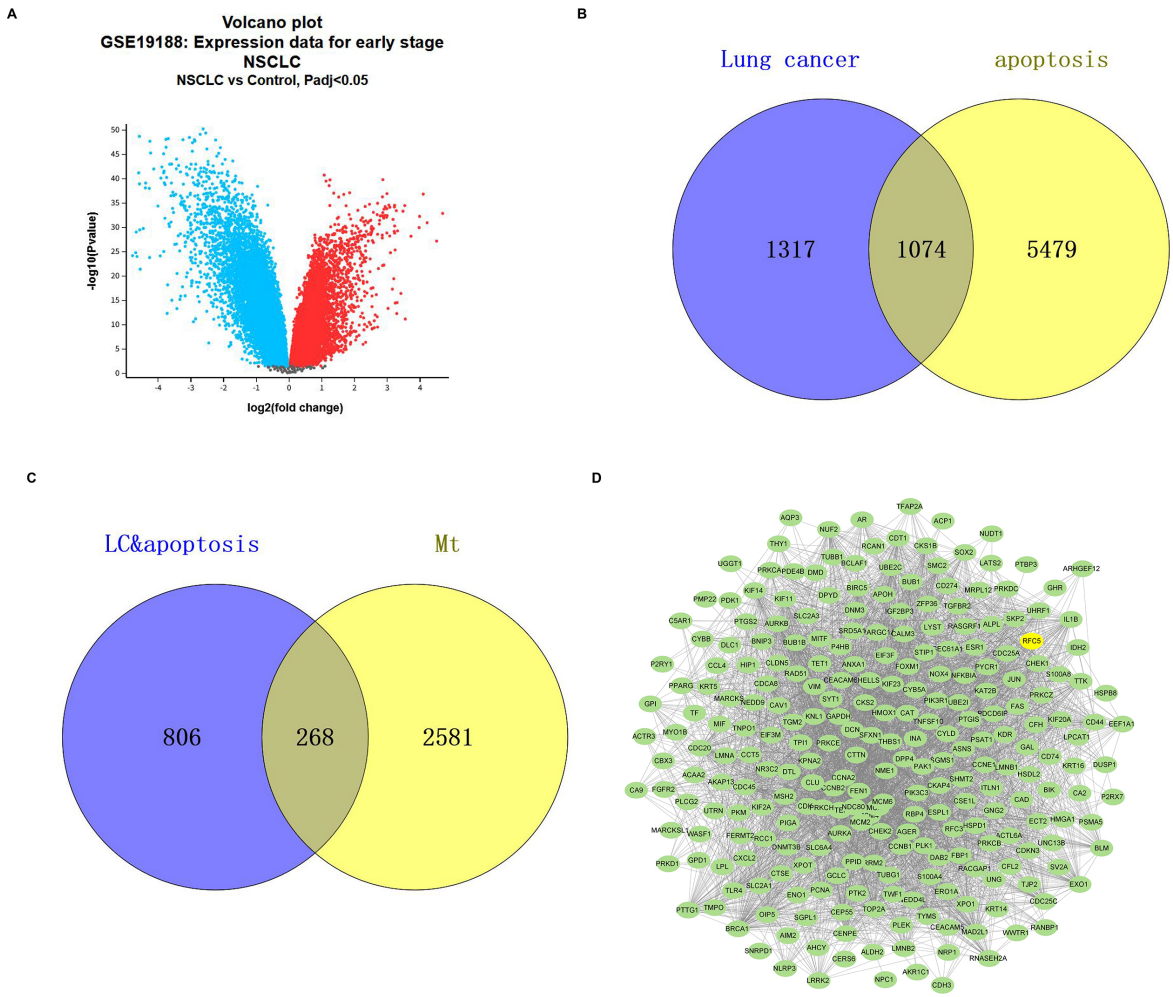

Fig. 1. Bioinformatic identification of replication factor C 5 (RFC5) in non-small cell lung cancer (NSCLC). (A) Differentially expressed genes (DEGs) in NSCLC from the GSE19188 dataset (thresholds: |log2(Fold Change)| >1; adjusted *p*-value < 0.05). (B) Overlap between NSCLC DEGs and apoptosis-related genes from the GeneCards database (Relevance score >1). (C) Intersection of apoptosis-related DEGs and mitochondrial dynamics-related genes (fission/fusion; Relevance score >1). (D) Protein-protein interaction (PPI) network of 268 intersecting genes from (C), constructed using the Search Tool for the Retrieval of Interaction Gene/Proteins (STRING) and visualized with Cytoscape.

[14,15]. Protein-protein interaction analysis revealed an association between RFC5 and cyclin-dependent kinase 1 (CDK1), supported by a strong positive correlation in lung cancer and a robust docking score, suggesting a direct interaction. CDK1 is known to phosphorylate DRP1 at Ser616, thereby enhancing its fission activity and promoting mitochondrial fragmentation [16,17].

Accordingly, we speculated that RFC5 interacts with CDK1 to upregulate its expression, leading to enhanced DRP1 phosphorylation at Ser616, increased mitochondrial fission, and suppressed apoptosis in NSCLC cells. This study aims to elucidate the RFC5-CDK1 axis as a potential mechanism underlying mitochondrial dysfunction and apoptosis evasion in lung cancer.

Materials and Methods

Bioinformatics Analysis

The transcriptomic dataset GSE19188, generated on the GPL570 platform, was downloaded from the Gene Expression Omnibus (GEO) (https://www.ncbi.nlm.nih.gov/gds). It encompasses 156 tumor and adjacent normal samples derived from 91 NSCLC patients. We identified differentially expressed genes (DEGs) using a threshold of |log2(fold change)| >1 and an adjusted *p*-value < 0.05. Gene sets associated with apoptosis, mitochondrial fission, and fusion were acquired from the GeneCards database (https://www.genecards.org/). Protein-protein interaction (PPI) networks were constructed via the Search Tool for the Retrieval of Interacting Genes/Proteins (STRING) database

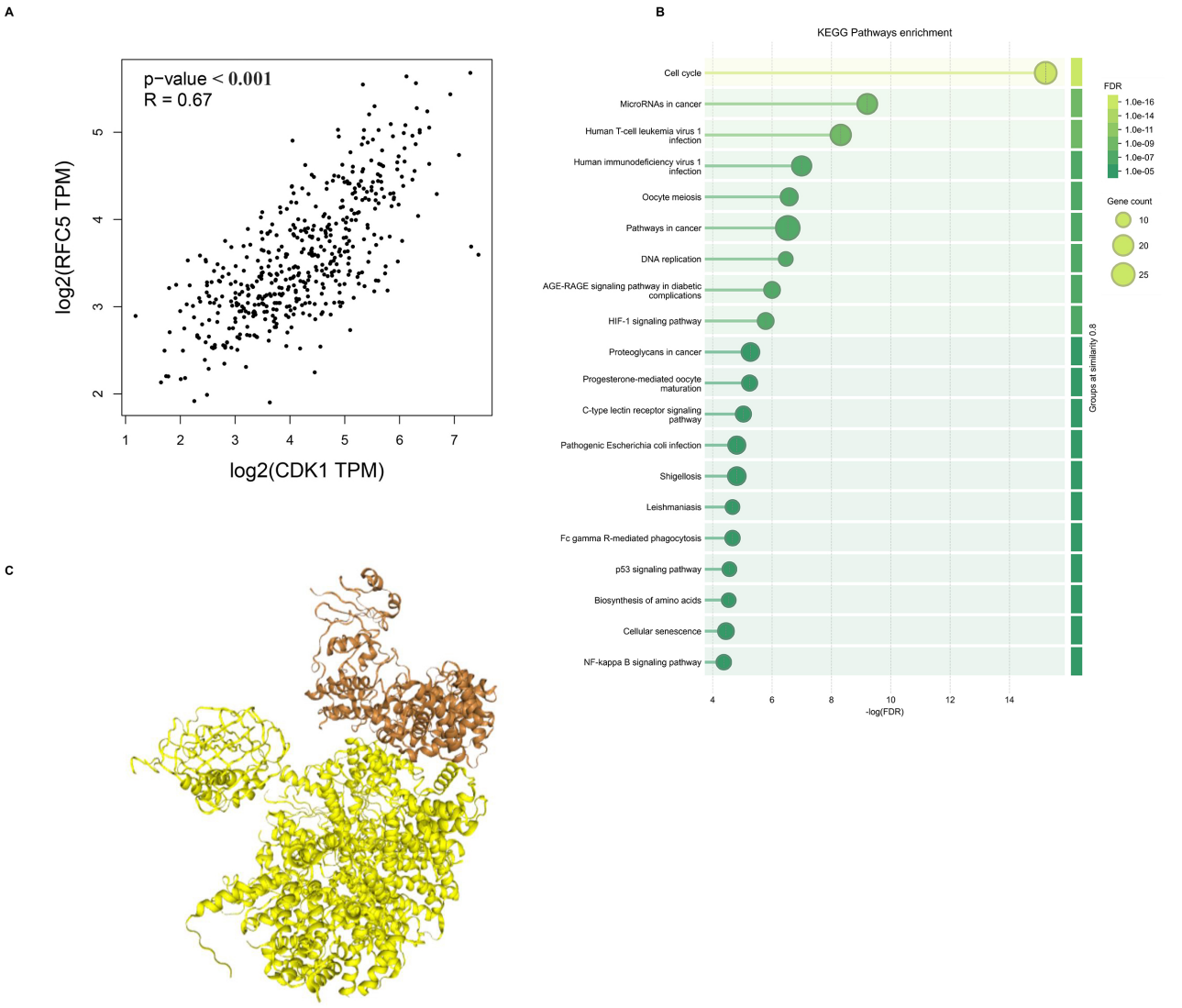

Fig. 2. The interaction between replication factor C5 (RFC5) and cyclin-dependent kinase 1 (CDK1) in NSCLC. (A) Correlation analysis between RFC5 and CDK1 mRNA expression in Lung Adenocarcinoma (LUAD) from the Gene Expression Profiling Interactive Analysis (GEPIA) database ($R = 0.67$, $p < 0.001$). (B) Kyoto Encyclopedia of Genes and Genomes (KEGG) pathway enrichment analysis of 268 candidate genes. (C) Molecular docking model predicting the binding conformation between RFC5 and CDK1.

(https://string-db.org/) (v11.5; minimum confidence score ≥0.95), with Cytoscape (v3.9.1) employed for visualization. Degree centrality was used to identify hub proteins. The correlation between RFC5 and CDK1 mRNA expression in lung adenocarcinoma (LUAD) was analyzed using GEPIA (http://gepia.cancer-pku.cn/); key parameter settings: dataset source = The Cancer Genome Atlas (TCGA) Tumor/Normal, expression unit = log2(TPM + 1), correlation was assessed using Pearson correlation coefficient. Kyoto Encyclopedia of Genes and Genomes (KEGG) pathway enrichment analysis was conducted using the clusterProfiler R package based on a hypergeometric test with multiple testing correction ($p < 0.05$).

Molecular Docking

The three-dimensional structures of human RFC5 and CDK1 proteins were downloaded from the AlphaFold database in PDB format. Molecular docking simulations were performed using HDOCK (http://huanglab.phys.hust.edu.cn/).

Cell Culture and Treatment

Human NSCLC cell line A549 (AW-CH0021, AnWei-sci, Shanghai, China) in Dulbecco's Modified Eagle Medium/Nutrient Mixture F-12 (DMEM/F-12) medium (BasMed-AW-005, AnWei-sci) supplemented with 10% fetal bovine serum (FBS; AW-FBS-001, AnWei-sci) and 1% Penicillin-Streptomycin (V900929, Sigma-Aldrich, St

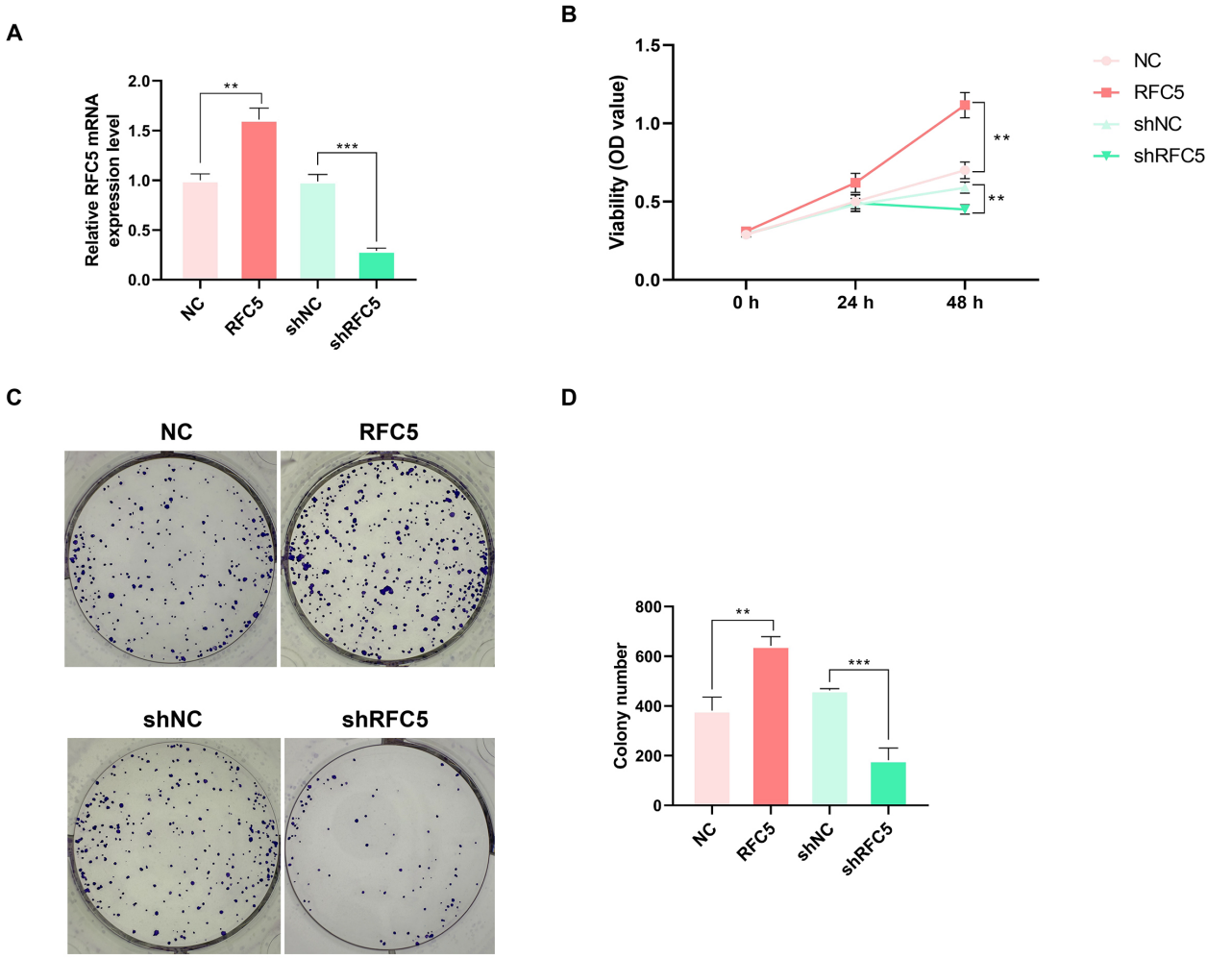

Fig. 3. RFC5 promotes NSCLC cell proliferation and viability. (A) Quantitative real-time PCR (qRT-PCR) analysis of RFC5 mRNA expression in A549 cells transfected with RFC5 overexpression vector (RFC5) or shRNA against RFC5 (shRFC5), with their respective negative controls (NC, shNC) (Glyceraldehyde-3-phosphate dehydrogenase (GAPDH) serves as an internal control). (B) A549 cell viability with RFC5 expression modulated at 24 and 48 hours (Cell Counting Kit-8). (C,D) A549 cell proliferation with modulated RFC5 expression (Colony formation assay). Values are the mean ± SD of three independent repeats; $^{**}p < 0.01$, $^{***}p < 0.001$.

Louis, MO, USA) was cultured in a humidified incubator (37 °C, 5% CO_2). Cells underwent authentication by short tandem repeat profiling and were confirmed to be free of mycoplasma contamination. For pharmacological inhibition, A549 cells were exposed to DRP1 inhibitor Mdivi-1 (25 µM; HY-15886, MedChemExpress, Monmouth Junction, NJ, USA) for 2 hours.

Cell Transfection

Overexpression vectors for RFC5 and CDK1 were constructed by inserting the full-length coding sequence of human RFC5 (NM_001130112.4, **Supplementary Materials**) and human CDK1 (NM_001170406.1, **Supplementary Materials**) into the pcDNA3.1(+) empty vector (VT1001, YouBio, Changsha, China), with the pcDNA3.1(+) empty vector as a negative control (NC). For gene knockdown, the pRNAT-U6.1/Neo plasmids harboring either short hairpin RNA against RFC5 (shRFC5, 5′-GTAACTATCTGTCAAAGAT-3′) or a non-targeting control (shNC, 5′-TTCTCCGAACGTGTCACGT-3′) were obtained from RiboBio in China. A549 cells (1×10^4/well) were transfected at 70–90% confluence using Lipo2000 Transfection Reagent (MX2211-1.50ML, Shanghai Maokang Biotechnology Co, Ltd., Shanghai, China). Transfection efficiency was confirmed by quantitative real-time PCR (qRT-PCR) after 48 hours of culture.

Cell Viability Assay

With Cell Counting Kit-8 (CCK-8; ab228554, Abcam, Cambridge, UK), A549 cells in 96-well plates (5×10^3/well) underwent respective treatments and were exposed to 10 µL WST-8 solution (4 hours, 37 °C). Absorbance (460 nm) was detected using a Multiskan^{TM} FC Microplate Photometer (Thermo Fisher Scientific,

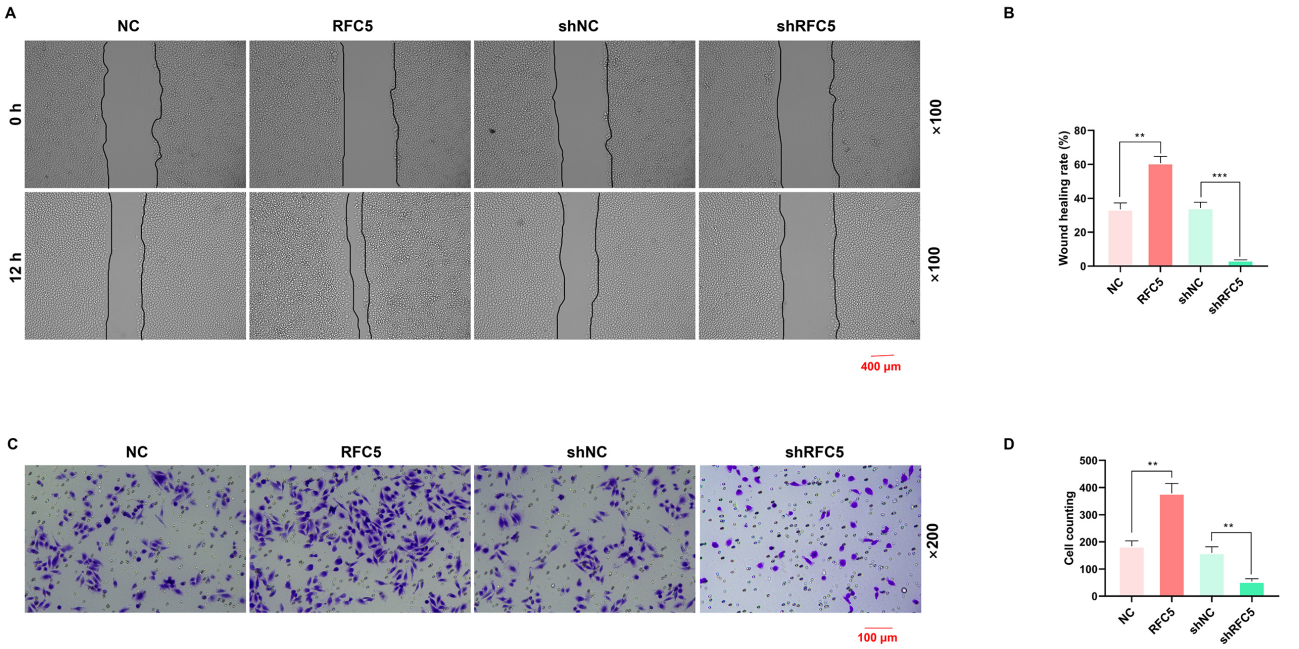

Fig. 4. RFC5 enhances NSCLC cell migratory and invasive capacities. (A,B) Wound healing assays in A549 cells with modulated RFC5 expression at 0- and 12- hour post-scratching. Scale = 400 μm (×100). (C,D) Cell invasion with modulated RFC5 expression (Transwell assays). Scale = 100 μm (×200). Values are the mean ± SD of three independent repeats; $^{**}p < 0.01$, $^{***}p < 0.001$.

Waltham, MA, USA).

Colony Formation Assay

1×10^3 A549 cells were seeded per dish and cultured for 10 days. Resulting colonies were fixed (4% paraformaldehyde; abs9179, Absin, Shanghai, China) and stained (0.01% Giemsa solution; abs47047618, Absin, China). Colonies exceeding 0.1 mm in diameter were counted automatically using a GelCount colony counter (Oxford Optronix, Oxford, UK).

Wound Healing Assay

A confluent monolayer of A549 cells cultured in a 6-well plate was uniformly scratched using a sterile 200-μL pipette tip. After scratching, the cells were gently washed with phosphate-buffered saline (PBS) to remove detached cells, and the culture medium was replaced with serum-free medium. Wound images were captured at 0- and 12- hour post-scratching using a BX53F microscope (100× magnification; OLYMPUS, Tokyo, Japan) to evaluate cell migration.

Cell Invasion Assay

Cell invasion assessment was conducted using Transwell inserts (8-μm pores; 140644, Thermo Fisher Scientific, USA) pre-coated with Matrigel (E1270, Sigma-Aldrich). Prior to the assay, 1×10^4 cells suspended in serum-free medium in the upper chamber were allowed to invade toward medium containing 10% FBS in the lower chamber. After 48 hours of incubation, cells that had migrated through the Matrigel-coated membrane were fixed, stained with Giemsa, and then imaged at ×200 magnification.

Apoptosis Analysis

Using an ApoDETECT Annexin V-fluorescein isothiocyanate (FITC) kit (331200, Thermo Fisher Scientific), treated cells were harvested, washed twice with cold PBS, and resuspended in 1× binding buffer at a density of approximately 1×10^6 cells/mL. Then, 100 μL of the cell suspension was transferred to a flow cytometry tube, followed by staining with 5 μL of Annexin V-FITC and 5 μL propidium iodide (PI; 15 minutes, room temperature, darkness). After staining, the samples were analyzed immediately on an Attune CytPix flow cytometer (Thermo Fisher Scientific).

Measurement of Mitochondrial Membrane Potential (MMP, ΔΨm)

ΔΨm was assessed using a JC-1 Assay Kit (C2003S, Beyotime, Shanghai, China). A549 cells were incubated with JC-1 staining solution (20 minutes, 37 °C). Fluorescence signals were captured under fluorescence microscopy (×200 magnification), with JC-1 aggregates (red fluorescence) indicating high ΔΨm and monomers (green fluorescence) indicating low ΔΨm. The red/green fluorescence intensity ratio was calculated to reflect ΔΨm levels.

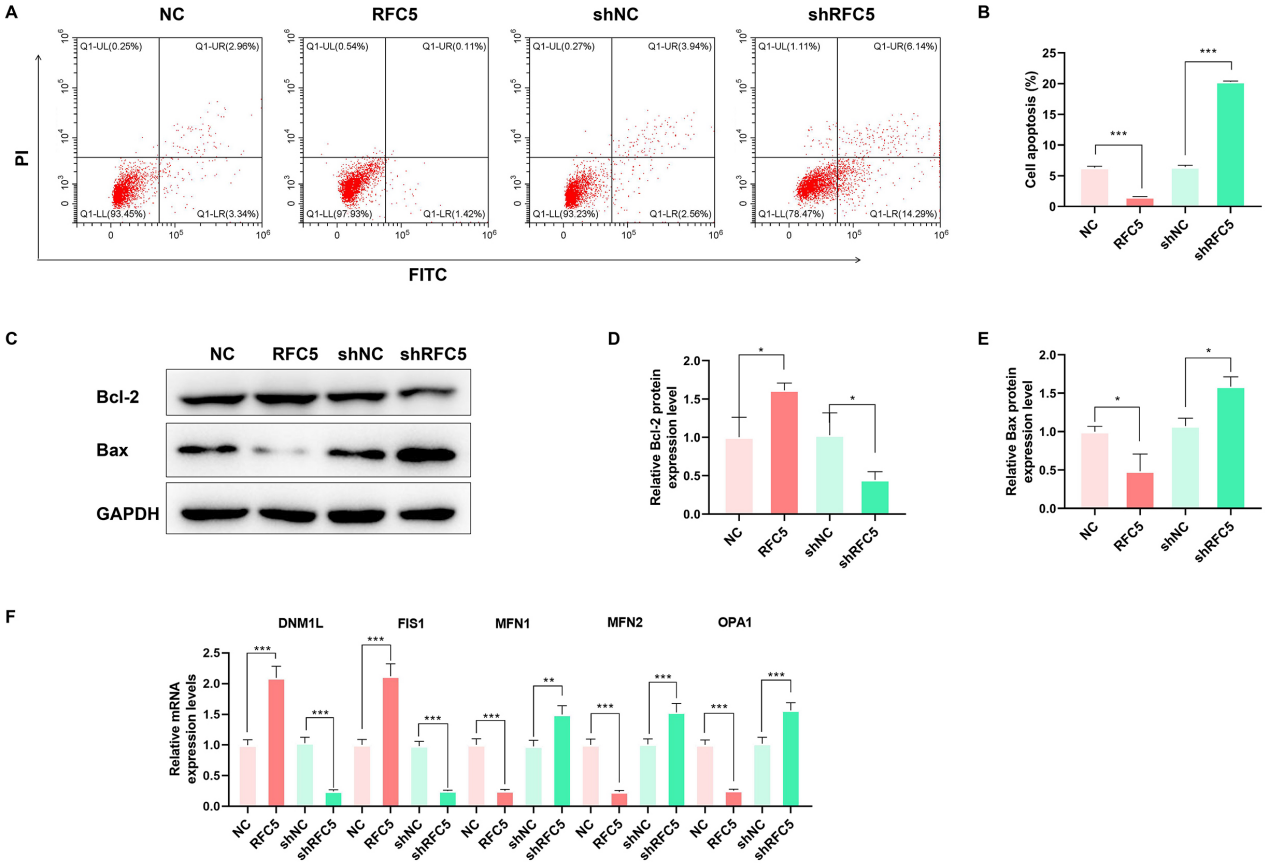

Fig. 5. RFC5 inhibits apoptosis and regulates mitochondrial dynamics-related gene expression. (A,B) Apoptosis in A549 cells with modulated RFC5 expression (flow cytometry and Annexin V/PI staining). (C–E) B-cell lymphoma 2 (Bcl-2) and BCL-2-associated X protein (Bax) protein levels (Western blot analysis), with GAPDH serving as a loading control. (F) Key mitochondrial dynamics gene (DNM1L, FIS1, MFN1, MFN2, OPA1) mRNA expression in A549 cells with modulated RFC5 expression (qRT-PCR analysis). Values are the mean ± SD of three independent repeats; *$p < 0.05$, **$p < 0.01$, ***$p < 0.001$.

Co-Immunoprecipitation (Co-IP)

Prepared A549 cell lysates were divided into input, IP, and IgG control groups. The IP and IgG samples were incubated overnight at 4 °C with either an anti-RFC5 antibody (10385-1-AP, 1:100, Proteintech Group, Wuhan, China) or non-specific IgG (ab172730, 1:100, Abcam, Cambridge, UK), respectively. Protein A/G magnetic beads (P2177S, Beyotime, China) were introduced and incubated for 1 hour. Following thorough rinsing with PBS containing 0.1% Tween-20 (PBS-T), bound proteins were eluted in loading buffer by heating at 95 °C (10 minutes) and underwent Western blot analysis.

Western Blot Analysis

Total protein was extracted from cells using Radio-Immunoprecipitation Assay (RIPA) Lysis Buffer (R0010, Solarbio, China) containing a protease and phosphatase inhibitor cocktail (P1261, Solarbio, Shanghai, China), followed by protein concentration determination with a Bicinchoninic Acid (BCA) Protein Assay Kit (PC0020, Solarbio, China). Following SDS-PAGE using NuPAGE™ 4–12% Bis-Tris gels (NP0321BOX, Thermo Fisher Scientific), proteins were transferred onto PVDF membranes (YA1701, Solarbio, China). Blocked membranes were incubated (overnight, 4 °C) with primary antibodies (Abcam): B-cell lymphoma 2 (Bcl-2; ab182858, 1:20,000), BCL-2-associated X protein (Bax; ab32503, 1:2000), and glyceraldehyde-3-phosphate dehydrogenase (GAPDH; ab9485, 1:2500; loading control), followed by incubation with corresponding horseradish peroxidase (HRP)-conjugated secondary antibody (ab175781, anti-rabbit, 1:10,000, Abcam). BeyoECL Plus reagent (P0018S, Beyotime, China) enabled band visualization on an iBright CL750 imaging system (Thermo Fisher Scientific). Band intensities were quantified with ImageJ software (v1.52s, NIH, Bethesda, MD, USA).

qRT-PCR

Following total RNA extraction (TRIzol™ Plus RNA Purification Kit; 12183555, Thermo Fisher Scientific) and reverse transcription into cDNA (SuperScript™ VILO™

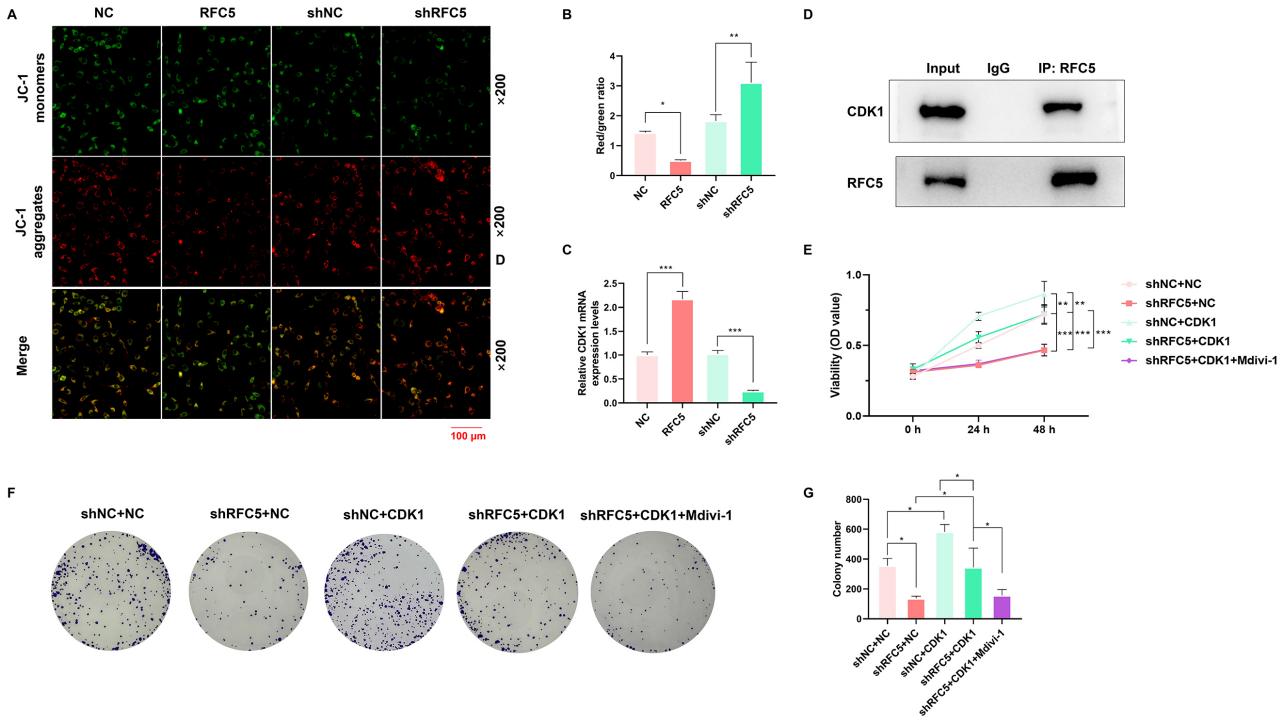

Fig. 6. RFC5 interacts with CDK1 and modulates mitochondrial function. (A,B) Mitochondrial membrane potential (ΔΨm) in A549 cells (immunofluorescence, JC-1 staining) (decreased red/green fluorescence ratio denotes depolarization). Scale=100 μm (×200). (C) CDK1 mRNA expression in A549 cells with modulated RFC5 expression (qRT-PCR analysis). (D) Physical interaction between RFC5 and CDK1 in A549 cell lysates (Co-immunoprecipitation). Input, IgG control, and IP with an anti-RFC5 antibody are shown. (E) Cell viability under different conditions: shRFC5, CDK1 overexpression, and treatment with the DRP1 inhibitor Mdivi-1 (25 μM) (CCK-8 assay). (F,G) Colony formation under the indicated treatment conditions. Values are the mean ± SD of three independent repeats; *$p < 0.05$, **$p < 0.01$, ***$p < 0.001$.

cDNA Synthesis Kit; 11754050, Thermo Fisher Scientific), Fast SYBR™ Green Master Mix (4385612, Thermo Fisher Scientific) and primers (Table 1) were employed for qRT-PCR on a QuantStudio™ 7 Pro Real-Time PCR System (Thermo Fisher Scientific). The cycling protocol consisted of 95 °C (20 sec), as well as 40 cycles of 95 °C (3 sec) and 60 °C (30 sec). Gene levels were normalized to GAPDH and calculated using the $2^{-\Delta\Delta Ct}$ method [18].

Statistical Analysis

For all experimental procedures, a minimum of three independent replicates were performed; results are expressed as mean ± standard deviation (SD); inter-group differences were evaluated using an unpaired two-tailed Student's *t*-test (two groups) or one-way analysis of variance (ANOVA) (multiple groups) followed by Tukey post-hoc test, with $p < 0.05$ denoting significance. All analyses were conducted using GraphPad Prism 8 software (GraphPad Software, Inc., San Diego, CA, USA).

Results

Bioinformatic Identification of RFC5 as a Potential Oncogene Interacting With CDK1 in NSCLC

To identify critical genes in NSCLC pathogenesis, GSE19188 dataset was examined, yielding 2391 DEGs using a threshold of |log2(Fold Change)| >1 and an adjusted *p*-value < 0.05 (Fig. 1A). Overlapping these DEGs with GeneCards database-derived apoptosis genes resulted in 1074 candidate genes (Fig. 1B). A further intersection with mitochondrial fission/fusion-related genes refined this list to 268 core genes (Fig. 1C). PPI network analysis of these 268 genes revealed a complex regulatory network, with RFC5 emerging as a node of interest (Fig. 1D). The GEPIA database further revealed a positive correlation between RFC5 and CDK1 mRNA expression in LUAD ($R = 0.67$, $p < 0.001$) (Fig. 2A). KEGG pathway enrichment analysis showed that these candidate genes were significantly involved in critical cancer-related pathways (Fig. 2B). Molecular docking simulations strongly supported a direct physical interaction between RFC5 and CDK1, with a high binding affinity (Fig. 2C).

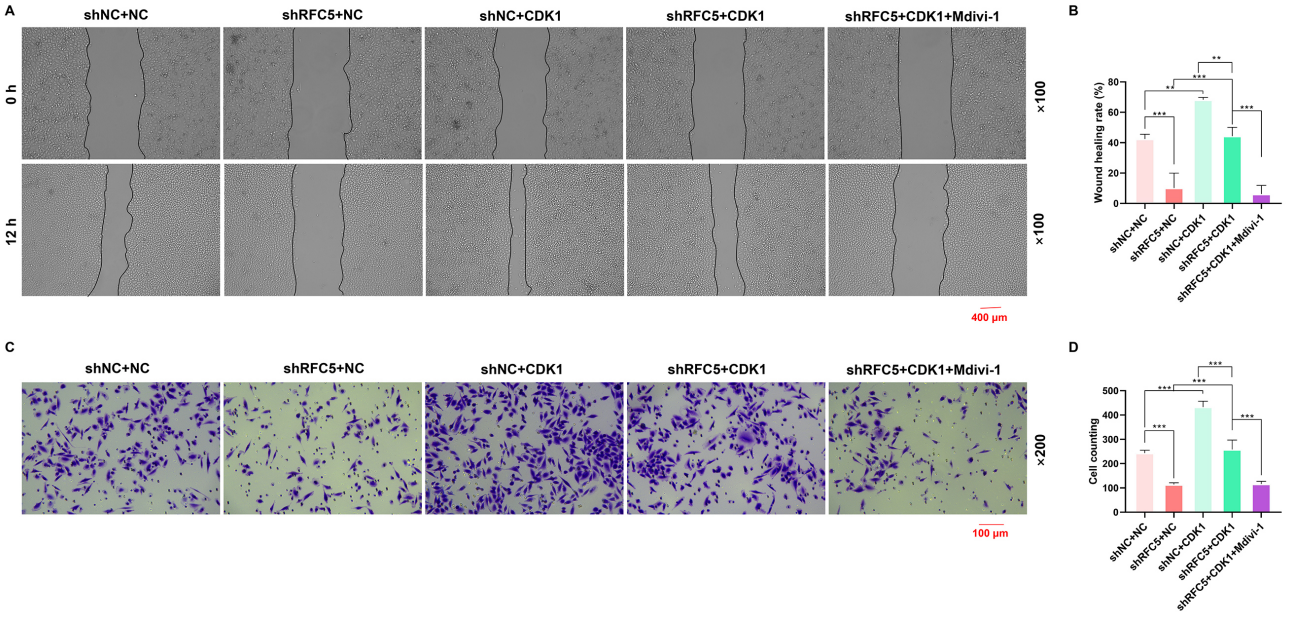

Fig. 7. The effects of CDK1 overexpression and DRP1 inhibition on the malignant phenotypes altered by RFC5 knockdown. (A,B) Wound healing under the indicated treatment conditions at 0 and 12 hours. Scale = 400 µm (×100). (C,D) Cell invasion under the indicated treatment conditions (Transwell assays). Scale = 100 µm (×200). Values are the mean ± SD of three independent repeats; **$p < 0.01$, ***$p < 0.001$.

Table 1. Primer sequences used in qRT-PCR.

Targets	Sense (5'-3')	Antisense (5'-3')
RFC5	AACTCTGAAGGGGTTGGCAC	CAGAGCATCTAGGCCTCTGC
DNM1L	GCTCCAGGACGTCTTCAACA	TCTGCTTCCACCCCATTTTCT
FIS1	GAAAGATGGACTCGTGGGCA	AGAACAGGGAAAGGACAGCG
MFN1	TGAGGCAGTTTGGCATCTGT	TCCGAGATAGCACCTCACCA
MFN2	GAAGGTGAAGCGCAATGTC	TGACAAAGTGCTTAAGTGGGG
OPA1	CTGTGGCCTGGATAGCAGAA	GCGAGGCTGGTAGCCATATT
GAPDH	AATGGGCAGCCGTTAGGAAA	GCGCCCAATACGACCAAATC

qRT-PCR, quantitative real-time PCR; *RFC5*, replication factor C 5; *DNM1L*, dynamin 1 like; *FIS1*, fission, mitochondrial 1; *MFN1*, Mitofusin 1; *OPA1*, optic atrophy protein 1; *GAPDH*, glyceraldehyde-3-phosphate dehydrogenase.

RFC5 Promotes NSCLC Malignant Phenotypes

Manipulation of RFC5 expression in A549 NSCLC cells was performed to elucidate its biological function. The qRT-PCR confirmed the efficient overexpression and knockdown of RFC5 (Fig. 3A; $p < 0.01$). Functional assays revealed that RFC5 overexpression significantly enhanced cell viability at 48 hours (Fig. 3B; $p < 0.01$) and proliferative capacity (Fig. 3C,D; $p < 0.01$). Conversely, RFC5 knockdown exerted the opposite effects (Fig. 3B–D; $p < 0.01$). Moreover, RFC5 overexpression promoted migration (Fig. 4A,B; $p < 0.01$) and invasion of A549 cells (Fig. 4C,D; $p < 0.01$), while RFC5 knockdown exerted the opposite effects (Fig. 4C,D; $p < 0.01$).

RFC5 Suppresses Apoptosis and Alters Mitochondrial Dynamics Gene Expression

Given the initial bioinformatic link to apoptosis, we examined how RFC5 influences cell death and found that RFC5 overexpression significantly inhibited apoptosis, while its knockdown promoted it (Fig. 5A,B; $p < 0.001$). This anti-apoptotic role was further corroborated by the finding that RFC5 upregulated Bcl-2 and downregulated Bax (Fig. 5C–E; $p < 0.05$). Furthermore, qRT-PCR analysis indicated that RFC5 upregulated mitochondrial fission genes (*DNM1L*, *FIS1*) and downregulated fusion genes (*MFN1*, *MFN2*, *OPA1*) (Fig. 5F; $p < 0.001$), suggesting a shift in mitochondrial dynamics towards fission. RFC5 knockdown exerted an opposite effect on the expression of these markers of apoptosis and mitochondrial dynamics (Fig. 5C–F; $p < 0.05$).

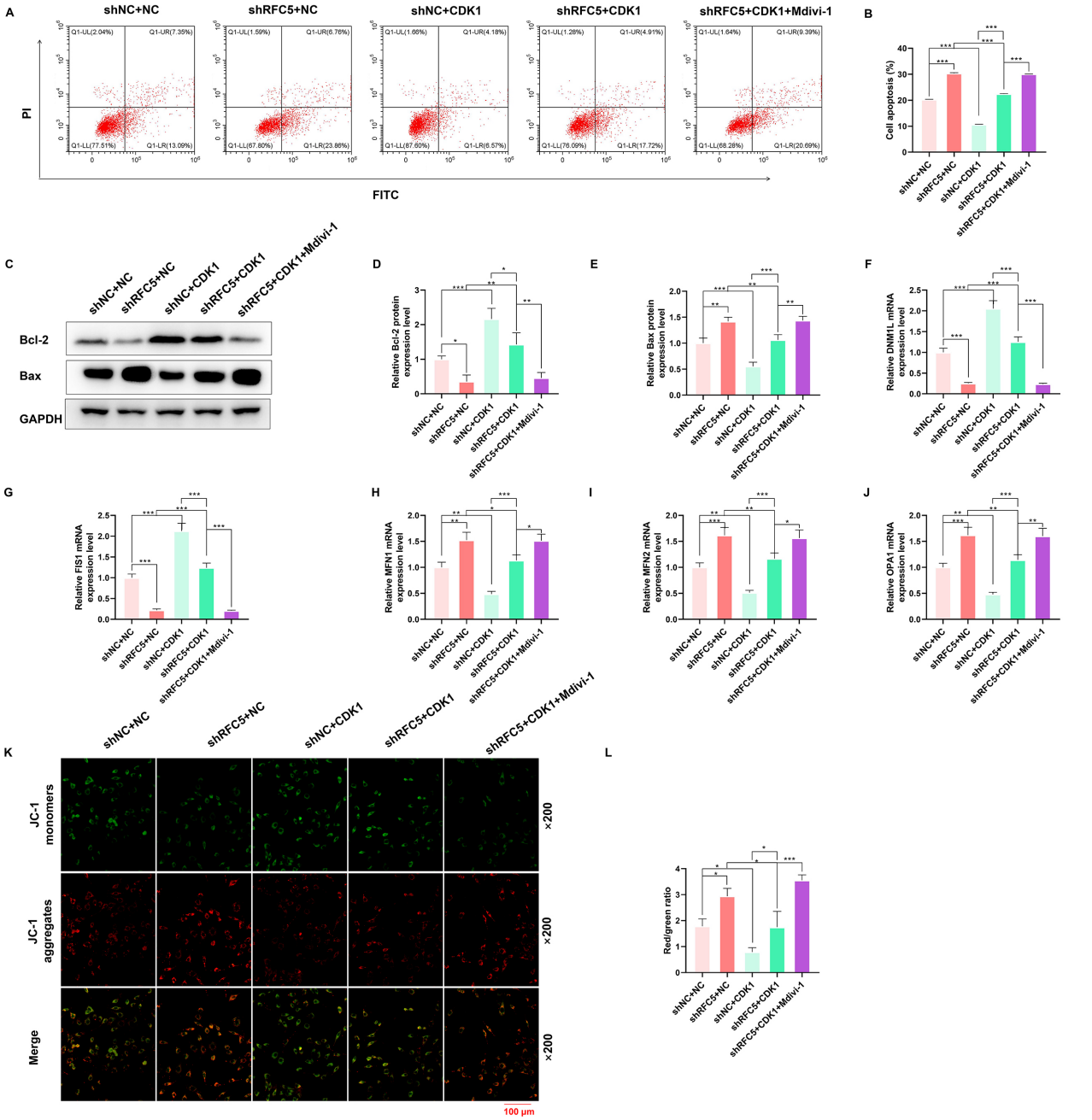

Fig. 8. The RFC5/CDK1 axis regulates apoptosis and mitochondrial dynamics via DRP1. (A,B) Apoptosis under the indicated treatment conditions (flow cytometry). (C–E) Bcl-2 and Bax protein levels (Western blot assays). (F–J) Mitochondrial dynamics-related gene (DNM1L, FIS1, MFN1, MFN2, OPA1) expression under the indicated treatment conditions (qRT-PCR analysis). (K,L) ΔΨm under the indicated treatment conditions (immunofluorescence). Scale = 100 μm (×200). Values are the mean ± SD of three independent repeats; *$p < 0.05$, **$p < 0.01$, ***$p < 0.001$.

RFC5 Interacts With CDK1 and Modulates MMP

We then validated the interaction between RFC5 and CDK1. JC-1 staining revealed that RFC5 overexpression reduced the ΔΨm, whereas knockdown increased it (Fig. 6A,B; $p < 0.05$). We confirmed that RFC5 positively regulates CDK1 at the mRNA level (Fig. 6C; $p < 0.001$). Critically, Co-IP assays physically confirmed the interaction between RFC5 and CDK1 in A549 cells (Fig. 6D).

The RFC5/CDK1 Axis Promotes Malignant Phenotypes via DRP1-Mediated Mitochondrial Fission

To delineate the functional cascade, we performed rescue experiments. Silencing RFC5 suppressed cell viability at 48 hours (Fig. 6E) and proliferation (Fig. 6F,G), and these effects were reversed by co-overexpression of CDK1 ($p < 0.05$). Importantly, the enhanced viability and prolif-

eration driven by CDK1 overexpression in the context of RFC5 knockdown were abolished by the DRP1 inhibitor Mdivi-1 (Fig. 6E–G, $p < 0.05$). A consistent pattern was confirmed in cell migration (Fig. 7A,B; $p < 0.01$) and invasion (Fig. 7C,D; $p < 0.001$).

The RFC5/CDK1/DRP1 Signaling Axis Regulates Apoptosis and Mitochondrial Function

The results demonstrated that the pro-apoptotic effect of RFC5 knockdown was rescued by CDK1 overexpression, and this rescue was again negated by Mdivi-1 (Fig. 8A,B; $p < 0.001$). Expression analysis of Bcl-2 and Bax confirmed these findings at the protein level (Fig. 8C–E; $p < 0.05$). Similarly, the alterations in mitochondrial dynamics-related gene expression (Fig. 8F–J) and ΔΨm (Fig. 8K,L) induced by RFC5 knockdown were all reversed by CDK1 overexpression, and these reversals were blocked upon DRP1 inhibition with Mdivi-1 ($p < 0.05$).

Discussion

This research, based on *in vitro* experiments, highlights the importance of RFC5 in NSCLC progression, potentially by activating CDK1-dependent mitochondrial fragmentation. Our findings delineate a linear signaling pathway wherein RFC5, traditionally recognized as a DNA replication factor, physically interacts with and upregulates CDK1, which in turn enhances DRP1-mediated mitochondrial fission, ultimately suppressing apoptosis and conferring aggressive malignant phenotypes. This study not only expands the functional repertoire of RFC5 beyond the nucleus but also preliminarily suggests a mechanistic link between DNA replication machinery and mitochondrial dynamics in NSCLC based on *in vitro* cellular findings.

Our most notable finding is a direct interaction between RFC5 and CDK1. While both proteins are established regulators of the cell cycle, their functional interaction in NSCLC pathogenesis remains largely unexplored. Our bioinformatic analysis revealing a strong positive correlation, coupled with robust molecular docking and co-immunoprecipitation data, provides compelling evidence for their physical association. This interaction suggests that RFC5 may serve as a regulatory subunit or a stabilizing partner for CDK1, thereby enhancing its kinase activity. The key role of CDK1 in this axis is further underscored by its established function in catalyzing DRP1 phosphorylation at Ser616, a key step in promoting mitochondrial fission [16,17].

Our findings resonate with and extend the mounting supporting data highlighting mitochondrial dynamics as key drivers of cancer progression. The mitochondrial fission/fusion equilibrium can mediate tumor cell behavior [19,20,21,22]. Herein, we revealed a dual regulatory effect of RFC5 on mitochondrial dynamics, characterized by the upregulation of fission mediators (*DNM1L*, *FIS1*) and concurrent downregulation of fusion regulators (*MFN1*, *MFN2*, *OPA1*), effectively shifting the mitochondrial equilibrium towards a fragmented state. This mechanism was functionally supported by ΔΨm and reduced apoptosis upon RFC5 overexpression. This pro-fission state is not unique to our model; recent studies have shown that circ0515 also reprograms mitochondrial metabolism and dynamics to accelerate NSCLC progression and invasion [23]. Our findings position the RFC5-CDK1 axis as another crucial upstream regulator of this fundamental process.

The functional outcomes of activating the RFC5-CDK1-DRP1 axis—enhanced proliferation, migration, invasion, and apoptosis evasion—are hallmarks of cancer. Previous studies indicated that mitochondrial fragmentation enhances the migratory and invasive potential of tumor cells [24,25]. By linking RFC5 to this process, we provide a plausible explanation for its association with aggressive clinicopathological features in NSCLC. The anti-apoptotic effect, mediated through the Bcl-2/Bax rheostat, underscores how mitochondrial fission directly influences cell survival decisions. Our rescue experiments using the DRP1 inhibitor Mdivi-1 provided strong mechanistic evidence, positioning DRP1 as the non-redundant, terminal executor of this signaling axis. The complete abrogation of CDK1's rescue effect by Mdivi-1 confirms that the oncogenic functions of the RFC5-CDK1 axis are critically dependent on DRP1-mediated mitochondrial fission.

From a translational perspective, our study suggests the RFC5-CDK1 axis represented a novel therapeutic vulnerability in NSCLC. This insight is particularly relevant given the rapid evolution of treatment paradigms, in which combinations of different therapeutic modalities are emerging as promising strategies. For example, the combination of TROP2-directed Antibody-Drug Conjugates (ADCs) with immune checkpoint inhibitors has recently demonstrated impressive efficacy in driver-gene negative advanced NSCLC, potentially offering a new treatment option for this patient population [26]. Furthermore, innovative prognostic models that integrate features like programmed cell death and organelle function are paving the way for more personalized treatment strategies [27,28]. In this context, targeting mitochondrial fission, particularly in tumors with high RFC5/CDK1 activity, holds promise to overcome apoptosis resistance and potentially synergize with existing therapies, including immunotherapy and anti-angiogenic agents [29,30].

Despite these valuable findings, several limitations should be acknowledged. First, the detailed binding domains of the RFC5-CDK1 interaction and the direct regulatory effect of RFC5 on CDK1 kinase activity require further structural and biochemical validation. Second, we did not detect DRP1 phosphorylation level at Ser616, a canonical CDK1-targeted site responsible for DRP1 activation. The lack of p-DRP1 Ser616 data weakens the direct evidence for the RFC5-CDK1-DRP1 signaling cascade. Future studies

will include assessment of p-DRP1 Ser616 to verify CDK1-mediated activation of DRP1 and further strengthen the reliability of this signaling axis. Third, as this study was performed exclusively in the LUAD-derived A549 cell line, and given the heterogeneity of NSCLC subtypes, the generalizability of the RFC5-CDK1 axis across different NSCLC subtypes requires further validation using additional cell lines (e.g., H1703, H1299, SK-MES-1). Fourth, while we used the DRP1 inhibitor Mdivi-1 to implicate DRP1 in the RFC5-CDK1 axis, existing studies suggest Mdivi-1 may exert DRP1-independent effects [31,32]. Therefore, future studies using genetic knockdown of DRP1 (e.g., siRNA or CRISPR) are needed to confirm the specific dependency on DRP1-mediated mitochondrial fission in this signaling axis.

Conclusion

In conclusion, our *in vitro* research provides preliminary experimental evidence for a potential RFC5-CDK1 regulatory cascade that may contribute to NSCLC progression by modulating mitochondrial dynamics and suppressing cell apoptosis. This candidate pathway may represent a promising avenue for future mechanistic and therapeutic exploration in NSCLC. Therapeutic strategies that disrupt the interaction between RFC5 and CDK1 or inhibit downstream DRP1 activation may potentially become effective approaches for treating this malignant tumor.

Availability of Data and Materials

The analyzed datasets generated during the study are available from the corresponding author on reasonable request.

Author Contributions

YHH and YFD designed the research study; ZYR performed the research; ZHX collected and analyzed the data. QW contributed to data analysis and interpretation and drafted the manuscript. All authors have been involved in revising the manuscript critically for important intellectual content. All authors gave final approval of the version to be published. All authors have participated sufficiently in the work to take public responsibility for appropriate portions of the content and agreed to be accountable for all aspects of the work in ensuring that questions related to its accuracy or integrity.

Ethics Approval and Consent to Participate

Not applicable.

Acknowledgment

Not applicable.

Funding

This research received no external funding.

Conflict of Interest

The authors declare no conflict of interest.

Supplementary Material

Supplementary material associated with this article can be found, in the online version, at https://doi.org/10.24976/Discov.Med.202638210.170.

References

[1] Bray F, Laversanne M, Sung H, Ferlay J, Siegel RL, Soerjomataram I, et al. Global cancer statistics 2022: GLOBOCAN estimates of incidence and mortality worldwide for 36 cancers in 185 countries. CA: a Cancer Journal for Clinicians. 2024; 74: 229–263. https://doi.org/10.3322/caac.21834

[2] Li X, Jin L, Ma Y, Jiang Z, Tang H, Tong X. Xanthohumol inhibits non-small cell lung cancer by activating PUMA-mediated apoptosis. Toxicology. 2022; 470: 153141. https://doi.org/10.1016/j.tox.2022.153141

[3] Tang M, Xu M, Wang J, Liu Y, Liang K, Jin Y, et al. Brain Metastasis from EGFR-Mutated Non-Small Cell Lung Cancer: Secretion of IL11 from Astrocytes Up-Regulates PDL1 and Promotes Immune Escape. Advanced Science (Weinheim, Baden-Wurttemberg, Germany). 2024; 11: e2306348. https://doi.org/10.1002/advs.202306348

[4] Tao JH, Ren L, Chen HY, Feng SY. Exploring acupuncture therapy for dual-heart disease based on Zongqi theory and mitochondrial dysfunction. Journal of Basic Chinese Medicine. 2025; 31: 308–312. (In Chinese)

[5] Cheng X, Wang Y, Johnson B, You M. Mitochondria-targeted strategies in tumor immunity. Frontiers in Immunology. 2025; 16: 1646138. https://doi.org/10.3389/fimmu.2025.1646138

[6] Chen W, Zhao H, Li Y. Mitochondrial dynamics in health and disease: mechanisms and potential targets. Signal Transduction and Targeted Therapy. 2023; 8: 333. https://doi.org/10.1038/s41392-023-01547-9

[7] Zeng Z, You M, Fan C, Rong R, Li H, Xia X. Pathologically high intraocular pressure induces mitochondrial dysfunction through Drp1 and leads to retinal ganglion cell PANoptosis in glaucoma. Redox Biology. 2023; 62: 102687. https://doi.org/10.1016/j.redox.2023.102687

[8] Chen S, Sun Y, Qin Y, Yang L, Hao Z, Xu Z, et al. Dynamic interaction of REEP5-MFN1/2 enables mitochondrial hitchhiking on tubular ER. The Journal of Cell Biology. 2024; 223: e202304031. https://doi.org/10.1083/jcb.202304031

[9] Liang FG, Zandkarimi F, Lee J, Axelrod JL, Pekson R, Yoon Y, et al. OPA1 promotes ferroptosis by augmenting mitochondrial ROS and suppressing an integrated stress response. Molecular Cell. 2024; 84: 3098–3114.e6. https://doi.org/10.1016/j.molcel.2024.07.020

[10] Zanfardino P, Amati A, Perrone M, Petruzzella V. The Balance of MFN2 and OPA1 in Mitochondrial Dynamics, Cellular Homeostasis, and Disease. Biomolecules. 2025; 15: 433. https://doi.org/10.3390/biom15030433

[11] Li Y, Zhou B, Yang Y, Liu K, Zhou S. Dynorphin B induces mitochondrial fragmentation in NSCLC through the PKD/DRP-1 signaling pathway. Neuropeptides. 2025; 112: 102535. https://doi.org/10.1016/j.npep.2025.102535

[12] Mishra SR, Mishra P, Senapati PK, Mahapatra KK, Bhutia SK. Intricate role of DRP1 and associated mitochondrial fission signaling in carcinogenesis and cancer progression. Biochimica et Biophysica Acta. Reviews on Cancer. 2025; 1880: 189453. https://doi.org/10.1016/j.bbcan.2025.189453

[13] Wang N, Wang X, Lan B, Gao Y, Cai Y. DRP1, fission and apoptosis. Cell Death Discovery. 2025; 11: 150. https://doi.org/10.1038/s41420-025-02458-0

[14] Yao H, Zhou X, Zhou A, Chen J, Chen G, Shi X, et al. RFC5, regulated by circ_0038985/miR-3614-5p, functions as an oncogene in the progression of colorectal cancer. Molecular Carcinogenesis. 2023; 62: 771–785. https://doi.org/10.1002/mc.23523

[15] Chen H, Xie H, Zhang Y, Wang G. Construction of a prognostic signature of RFC5 immune-related genes in patients with cervical cancer. Cancer Biomarkers : Section a of Disease Markers. 2023; 37: 261–277. https://doi.org/10.3233/CBM-220347

[16] Lai YS, Chang CC, Chen YY, Nguyen TMH, Xu J, Chen YC, et al. Optogenetically engineered Ca2+ oscillation-mediated DRP1 activation promotes mitochondrial fission and cell death. Journal of Cell Science. 2023; 136: jcs260819. https://doi.org/10.1242/jcs.260819

[17] Li B, Liu L. Fibroblast growth factor 21, a stress regulator, inhibits Drp1 activation to alleviate skeletal muscle ischemia/reperfusion injury. Laboratory Investigation; a Journal of Technical Methods and Pathology. 2022; 102: 979–988. https://doi.org/10.1038/s41374-022-00787-7

[18] Su Y, Wang Y, Yu Q, Wu Z, Zhang D, Yan C. Eugenol suppresses VEGF-dependent angiogenesis by JAK2/STAT3 pathway in non-small cell lung cancer. Guidelines and Standards of Chinese Medicine. 2024; 2: 80–90.

[19] Zhao Z, Ren Y, Yuan M, Liu G, Sun J. The molecular mechanisms of mitochondrial dynamics and mitophagy and their complex association with cancer drug resistance. Journal of Translational Medicine. 2025; 23: 1047. https://doi.org/10.1186/s12967-025-07078-x

[20] Boulton DP, Caino MC. Mitochondrial Fission and Fusion in Tumor Progression to Metastasis. Frontiers in Cell and Developmental Biology. 2022; 10: 849962. https://doi.org/10.3389/fcell.2022.849962

[21] Wu Z, Xiao C, Li F, Huang W, You F, Li X. Mitochondrial fusion-fission dynamics and its involvement in colorectal cancer. Molecular Oncology. 2024; 18: 1058–1075. https://doi.org/10.1002/1878-0261.13578

[22] Ding M, Shi R, Fu F, Li M, De D, Du Y, et al. Paeonol protects against doxorubicin-induced cardiotoxicity by promoting Mfn2-mediated mitochondrial fusion through activating the PKCε-Stat3 pathway. Journal of Advanced Research. 2023; 47: 151–162. https://doi.org/10.1016/j.jare.2022.07.002

[23] Yuan Y, Wu Y, Li C, Huang Z, Peng D, Wu Z, et al. Circ0515 reprogramming mitochondrial succinate metabolism and promotes lung adenocarcinoma progression through regulating SDHB. Cell Death & Disease. 2025; 16: 497. https://doi.org/10.1038/s41419-025-07830-7

[24] Ma JT, Zhang XY, Cao R, Sun L, Jing W, Zhao JZ, et al. Effects of Dynamin-related Protein 1 Regulated Mitochondrial Dynamic Changes on Invasion and Metastasis of Lung Cancer Cells. Journal of Cancer. 2019; 10: 4045–4053. https://doi.org/10.7150/jca.29756

[25] Mo Y, Lin L, Zhang J, Yu C. SOAT1 enhances lung cancer invasiveness by stimulating AKT-mediated mitochondrial fragmentation. Biochemistry and Cell Biology = Biochimie et Biologie Cellulaire. 2022; 100: 68–74. https://doi.org/10.1139/bcb-2021-0175

[26] Zhang X, Jin Y, Lu J, Li N, Wu Z, Wu M, et al. Abstract 344: IBI3014, a TROP2xPD-L1 bi-specific ADC integrating ADC killing with checkpoint blockade within one molecule, exhibits promising efficacy and safety in preclinical models. Cancer Research. 2025; 85: 344.

[27] García-Pérez BE, Pérez-Torres C, Baltierra-Uribe SL, Castillo-Cruz J, Castrejón-Jiménez NS. Autophagy as a Target for Non-Immune Intrinsic Functions of Programmed Cell Death-Ligand 1 in Cancer. International Journal of Molecular Sciences. 2023; 24: 15016. https://doi.org/10.3390/ijms241915016

[28] Nagakannan P, Tabeshmehr P, Eftekharpour E. Oxidative damage of lysosomes in regulated cell death systems: Pathophysiology and pharmacologic interventions. Free Radical Biology & Medicine. 2020; 157: 94–127. https://doi.org/10.1016/j.freeradbiomed.2020.04.001

[29] Lee YG, Yang N, Chun I, Porazzi P, Carturan A, Paruzzo L, et al. Apoptosis: a *Janus bifrons* in T-cell immunotherapy. Journal for Immunotherapy of Cancer. 2023; 11: e005967. https://doi.org/10.1136/jitc-2022-005967

[30] Simayi N, Li J, Hu J, Jia N, Wan R, Xie J, et al. Bevacizumab and anlotinib combination therapy acts via HIF-1α suppression to exert synergistic anti-angiogenic and anti-tumor effects in non-small cell lung cancer. Frontiers in Immunology. 2025; 16: 1613368. https://doi.org/10.3389/fimmu.2025.1613368

[31] Ruiz A, Quintela-López T, Sánchez-Gómez MV, Gamindе-Blasco A, Alberdi E, Matute C. Mitochondrial division inhibitor 1 disrupts oligodendrocyte Ca^{2+} homeostasis and mitochondrial function. Glia. 2020; 68: 1743–1756. https://doi.org/10.1002/glia.23802

[32] Bordt EA, Clerc P, Roelofs BA, Saladino AJ, Tretter L, Adam-Vizi V, et al. The Putative Drp1 Inhibitor mdivi-1 Is a Reversible Mitochondrial Complex I Inhibitor that Modulates Reactive Oxygen Species. Developmental Cell. 2017; 40: 583–594.e6. https://doi.org/10.1016/j.devcel.2017.02.020